Effects of Post-Pyrolysis Air Oxidation on the Chemical Composition of Biomass Chars Investigated by Solid-State Nuclear Magnetic Resonance Spectroscopy

Xiaoyan Cao[1], Feng Xiao[2], Pu Duan[1], Joseph J. Pignatello[3], Jingdong Mao[4], Klaus Schmidt-Rohr[1,*]

[1] Department of Chemistry, Brandeis University, 415 South Street, Waltham, Massachusetts 02453, United States

[2] Department of Civil Engineering, University of North Dakota, Grand Forks, North Dakota 58202, United States

[3] Department of Environmental Sciences, The Connecticut Agricultural Experimental Station, New Haven, Connecticut 06511, United States

[4] Department of Chemistry and Biochemistry, Old Dominion University, 4541 Hampton Blvd, Norfolk, Virginia 23529, United States

Submitted to *Carbon*

Revised June 30, 2019

*Corresponding author. Tel: 781 736-2520. E-mail: srohr@brandeis.edu (Klaus Schmidt-Rohr)

Abstract

Solid-state nuclear magnetic resonance (NMR) spectroscopy was used to characterize the chemical changes induced by thermal air oxidation of biomass chars. Post-pyrolysis air oxidation (PPAO) was applied to anoxically-prepared maple wood and pecan shell chars at PPAO temperatures ranging from 300 to 600 ºC for up to 40 min. The ^{13}C NMR data showed that PPAO treatment introduced oxygen functionalities into aromatic rings, primarily C-O and C=O, but also carboxyl groups (COO) identified after spectral editing. The concentration of COO was relatively low (<3% of all C), consistent with potentiometric titration, and reached a discernable maximum slightly above 300 ºC. The COO enhancement from PPAO was lower than observed after wet-chemical oxidation with HNO_3 or ammonium persulfate. Concentrations of the C-O and C=O groups reached a maximum at PPAO temperatures between 350 and 400 ºC, and decreased at higher temperatures. These oxygen-containing functional groups were shown to generally increase with increasing PPAO time. Insight into the types and concentrations of oxygen functional groups induced by exposure of biomass chars to hot air has major implications for an understanding of the interaction of char with nutrients, natural organic matter, pollutants, and microbes, as well as electron transfer processes in soil.

1. INTRODUCTION

Chars are the carbonaceous products of incomplete combustion or pyrolysis of biomass and play a significant role in the global carbon cycle. They are ubiquitous in soil as a result of wildfires, land clearing, and crop-residue burning.[1-4] Oxidized chars contribute up to 80% of soil organic carbon in Amazonian Terra Preta soils, and 40-50% in dark, fertile Midwest prairie soils of the United States.[1, 5]. Their carboxylate (COO^-) groups can account for most of the cation exchange capacity of these soils.[5] The incorporation of fresh char produced by anoxic pyrolysis of biomass ("biochar") into soil has attracted attention in the agricultural and environmental communities for its potentially beneficial effects, such as carbon sequestration, improved soil fertility,[6, 7] suppression of nitrous oxide emissions,[8] and reduction in the mobility and bioavailability of chemical contaminants.[9]

The surface chemistry and pore characteristics of chars essential to their functions are affected by the biomass precursor materials [10] and, more importantly, the conditions (temperature–time heating profile) under which they are formed, produced, or weathered.[11-14] An important but less studied pyrolysis condition is ambient O_2 gas concentration.[15] Although fire-derived chars are typically exposed to a wide range of O_2 concentrations during their formation, engineered chars are generally produced from pyrolysis during which air is only occasionally introduced to the reactor to supplement energy input[16] or cool the reactor.[17] A few studies have reported the effects of thermal air oxidation (AO) after pyrolysis on the physical-chemical and adsorptive properties of chars. For instance, thermal AO has been considered as a step in the preparation of activated carbons from coal or nut shells[18-20], expanding pores and increasing surface area. It has also been shown to increase surface oxygen functionality, such as phenolic, carboxyl, and carbonyl groups.[21-24] Recent studies have shown that post-pyrolysis AO (PPAO) enhances the

adsorptive properties of biomass chars,[23, 24] possibly by removing pore wall matter and/or tarry deposits from pores ("reaming") or by creation of new acidic functionality for specific adsorptive sites.

Despite the potential benefits of thermal AO on adsorptive properties, the underlying chemical changes induced by oxidation are not well understood. For instance, characterization of the surface chemistry of air oxidized chars has mostly relied on X-ray photoelectron spectroscopy (XPS), Boehm titration, and Fourier transform infrared (FT-IR) spectroscopy,[21-24] which provide neither quantitative nor definitive information on oxygen-containing functional groups in chars. XPS of chars typically shows only one or two resolved peaks,[25] has an unresolved nonlinear baseline,[26] and cannot reliably quantify the composition of the whole sample since it probes merely the top few tens of nanometers of the sample. Solid-state nuclear magnetic resonance (NMR) spectroscopy is a powerful technique for characterizing chars because it is non-destructive and can provide comprehensive and quantitative composition information for the whole sample. Specifically, ^{13}C NMR spectroscopy can distinguish and quantify oxygen-containing functional group composition with respect to phenols/ethers, carboxyls/esters,[5] ketones/quinones, and aldehydes. NMR, unlike many other spectroscopies, is intrinsically quantitative and achieves small uncertainties of ± 0.5% of the total spectral area for peaks accounting for ~10% of the spectrum if direct polarization (DP) or multiple cross polarization (multiCP) is used with appropriate relaxation delays.[27, 28] The average fused ring size can also be estimated.[29] In the present study, we apply solid-state NMR spectroscopy to determine and quantify the chemical changes of biomass chars induced by PPAO. The air-oxidized char structure is compared with that of wet-chemically oxidized chars and with that of

natural oxidized char residues in soils. The effects of feedstock and of air oxidation temperature and duration are also investigated.

2. EXPERIMENTAL

2.1. Char Production and Oxidation

Maple wood char (MC) was prepared by heating wood shavings to 400 ºC in a flow of N_2 (1.5 L/min) and holding them at 400 ºC for 2 h. Pecan shell char (PC) was made anoxically from crushed shells at 400 ºC and provided by the United States Department of Agriculture (USDA)−Agricultural Research Service (ARS). PPAO was carried out by heating 0.1 g portions of char contained in 60 mL flat-bottom glass vials (diameter, 28 mm; height, 139 mm) open to the air in a muffle furnace at temperatures of 300, 350, 400, 500, or 600 ºC for 30 min. To evaluate the effect of PPAO time, chars were PPAO-treated at 400 ºC for 10, 20, 30 or 40 min. During the course of the PPAO process, the partial pressure of O_2 decreased from 0.2 bar to no less than 0.1 bar. The partial pressure of H_2O was below 0.05 bar. Further details of char preparation and oxidation have been described by Xiao and Pignatello.[24] The chars are denoted as MCxxx-yy or PCxxx-yy, where xxx corresponds to the PPAO temperature (ºC) and yy corresponds to the PPAO time (min). Under the PPAO conditions used, the MC400 and PC400 chars underwent ≤ 20% weight loss, depending on the PPAO time.[24]

The conversion of COOH to COOK groups, which results in a characteristic ^{13}C NMR chemical shift change of +7 ppm,[30, 31] was achieved by treating 100 mg of the MC350-30 char material suspended in deionized (DI) water with 0.1 M KOH. Titration to pH of 8.0 ensures deprotonation of COO groups, but not phenols, in the material. The treated char material was

washed three times with 1 mL of 0.1 M KOH and pelleted by centrifugation. After washing with DI water, the material was freeze-dried.

The PC350-30 char materials (~150 mg) were also oxidized separately with HNO_3 or ammonium persulfate (APS) following literature methods.[32] A saturated APS solution was prepared by adding an excess amount of APS (~75 g) to 100 mL of 1 M H_2SO_4. After 48 h of stirring, the saturated APS solution was filtered using a 0.22 μm filter (Millipore) and the filtrate was used for char oxidation. Briefly, ~15 mL of APS or 4 M HNO_3 were added to a glass pressure tube containing ~150 mg of char material, and the mixture was continuously stirred for 8.5 h at 120 ºC in an oil bath. Each oxidized char was removed from solution through 1.5 μm filter paper and rinsed with DI water until the pH of the filtrate was neutral. The filtered and rinsed chars were then freeze-dried.

2.2. Quantitative ^{13}C NMR Analysis

All NMR experiments were performed at 100 MHz for ^{13}C and 400 MHz for ^{1}H using a Bruker Avance 400 spectrometer equipped with a 4-mm double-resonance probe head. The ^{13}C chemical shifts were referenced to tetramethylsilane, using the COO resonance of glycine in the crystalline α-modification at 176.46 ppm as a secondary reference. Nearly quantitative ^{13}C NMR spectra were obtained by an improved, composite-pulse multiple cross polarization (multiCP) technique.[28] The modified multiCP pulse sequence replaced the direct 90º pulse in the conventional multiCP pulse sequence [27] with non-orthogonal phase 90º-180º pulses to reduce ^{13}C magnetization loss due to pulse imperfections. The multiCP experiments used a recycle delay of 0.7 s, ten 86-100% ^{1}H-amplitude ramp CP periods of 1.1 ms (and one of 0.55 ms duration) separated by 0.4 s delays for ^{1}H repolarization.

With a documented ± 5% relative uncertainty of the intensity of a given peak in a multiCP spectrum,[28] a peak of 10% intensity has an 'absolute' uncertainty of ± 5% × 10% = ± 0.5%. Part of the ± 5% error is systematic, affecting the signal of a given type of carbon in different samples in the same way, so the *trend* with PPAO temperature or time is even less uncertain.

From the fractional peak area (e.g., (5.0 ± 0.3)% of C=O carbon) and the total mass of carbon in the sample (easily calculated by multiplying the sample mass with the carbon content from elemental analysis; e.g., 40 mg C), one can specify the quantity of C=O carbon; in our example, it would be (5.0 ± 0.3)% × 40 mg C = (2.0 ± 0.1) mg C, corresponding to an amount of (0.17 ± 0.01) mmol C=O in the sample. Note that only the correct *fractional* peak areas (relative abundances) were required in the calculation. This means that any NMR processes that scale all peaks equally (e.g., spin-diffusion-homogenized $T_{1\rho}$ relaxation of ^{1}H magnetization during multiCP) will not interfere with quantification of the C=O carbons ("2.0 mg C", "0.17 mmol C=O") as outlined above.

In chars and other forms of black carbon, conductivity, diamagnetism, and unpaired electrons may create challenges to quantitative NMR. Fortunately, the pyrolysis temperature of the materials studied here was so low that conductivity did not interfere with NMR; specifically, no significant increase in the width of the electronic resonances of the probe head was observed, consistent with previous studies.[33] Diamagnetic broadening has been identified as a serious challenge to the observability of graphite NMR signal,[34] but even the moderate separation of graphene sheets due to intercalated ions is sufficient to greatly reduce this problem.[34] The fused ring systems generated by pyrolysis at 400 ^{o}C are fairly small [33], as shown by the significant fraction of C-H and C-O sheet-edge carbons, and the material is not graphitizable, i.e. the ring systems do not stack as in graphite,[35, 36] so the diamagnetic effect will remain small.

Coupling to unpaired electrons may make some nuclei unobservable by NMR. A hallmark of a significant concentration of unpaired electrons is fast spin lattice relaxation with $T_{1C} < 5$ s for all carbon sites.[37] However, this was not observed in the char samples studied here, which is consistent with a previous study [15] that reported shortened T_{1C} only in chars made by pyrolysis at ≥ 500 ºC. This matches with EPR studies in the literature, which have shown that the radical concentration increases strongly only above a pyrolysis temperature of 400 °C.[38] Signal loss due to unpaired electrons was quite insignificant in MC400-40 according to spin counting using direct polarization, which is particularly reliable[39] since the overall intensity is not affected by $T_{1\rho}$ relaxation of ^{1}H, unlike in multiCP NMR. Figure S1 compares spectra of MC400-40 obtained with 280-s DP and multiCP ^{13}C NMR, recorded in 47 and 8 hours, respectively. The spectra are in good agreement, confirming that multiCP provides correct fractional peak areas, with a much better signal-to-noise ratio than DP. Spin counting in turn demonstrates that the DP spectrum reflects (81 ± 15)% of the carbon in the sample. This quantification analysis was achieved by comparison of the DP ^{13}C NMR intensities of MC400-40 and of the methyl signals of Boc-alanine. In the analysis, the carbon masses were taken into account, as obtained by multiplying each sample mass in the NMR rotor with the carbon mass fraction (74 wt% C in MC400-40 from elemental analysis and 51 wt% C in Boc-alanine [27] from its chemical formula).

2.3. ^{13}C NMR Spectral Editing

Nonprotonated and mobile fractions were identified by applying a period of recoupled dipolar dephasing of 68 μs to dephase magnetization of carbons with strong dipolar couplings to ^{1}H, such as in immobile CH and CH_2 groups. To enhance the signals of COO groups relative to those

of aromatic carbons based on their smaller chemical-shift anisotropy,[40] total suppression of spinning sidebands (TOSS)[41] was applied at 4 kHz magic-angle spinning (MAS). The dynamic range of the COO signal was further improved by gated decoupling of 40 μs duration, which removed the aromatic C-H peak.

Long-range $^{13}C\{^{1}H\}$ dephasing can be used to assess the dipolar couplings of ^{1}H to aromatic carbons, which decrease as the size of the aromatic domains increases. Therefore, this method is useful for estimating the size of condensed aromatic clusters. This technique has usually been performed after direct polarization (DP), which provides relatively low sensitivity due to long recycle delays between scans.[29] Here we combined long-range C-H dephasing with multiCP instead of DP excitation. Given the shorter recycle delays and signal enhancement in multiCP, this allows for the spectra to be recorded with much enhanced signal-to-noise ratios. As a result, the peak positions and line shapes of the interior carbons can be determined more precisely. To detect nonprotonated carbons with good relative efficiency, multiCP and total suppression of spinning sidebands were used at a spinning frequency of 7 kHz, with a recycle delay of 1 s, ten 0.55 ms and one 1.1 ms 86-100% ramp CP periods, and a 0.3 s delay for ^{1}H repolarization. The ^{13}C 90º and 180º-pulse lengths were 4.2 and 8.4 μs, respectively, and ^{1}H 90º-pulse length was 4.3 μs. These experiments were performed for MC, MC400-20, MC400-30, and MC400-40.

3. RESULTS AND DISCUSSION

3.1. Effects of PPAO Temperature

The ^{13}C NMR spectrum of untreated maple wood char (MC, Fig. 1a, thick line) contained a major aromatic carbon peak, with a distinct shoulder at ~150 ppm arising from aromatic C-O in furans or phenols.[42] The minor signals in the alkyl region arose primarily from CH_3 and some

from CH_2/CH groups. The selective spectrum of nonprotonated C and CH_3 (thin line) indicates that the fraction of nonprotonated aromatic C-C is large (~54% of all C). The presence of significant signals for C=O in ketones or quinones between 174 and 220 ppm is also noteworthy. Spectral changes after PPAO treatment for 30 minutes at different temperatures are evident (Figs. 1(b-g)). Compared to the untreated maple wood char, the alkyl C (mainly CH_3) intensities decreased with increasing temperature. The aromatic C-O shoulder or peak near 155 ppm became better resolved with increasing temperature but decreased in intensity beyond MC400-30. Its intensity change was accompanied by a corresponding change in the signal intensity near 110 ppm, which can be assigned to aromatic carbons two bonds away from O; both signals reach a maximum in MC400-30 (Fig. 1g).

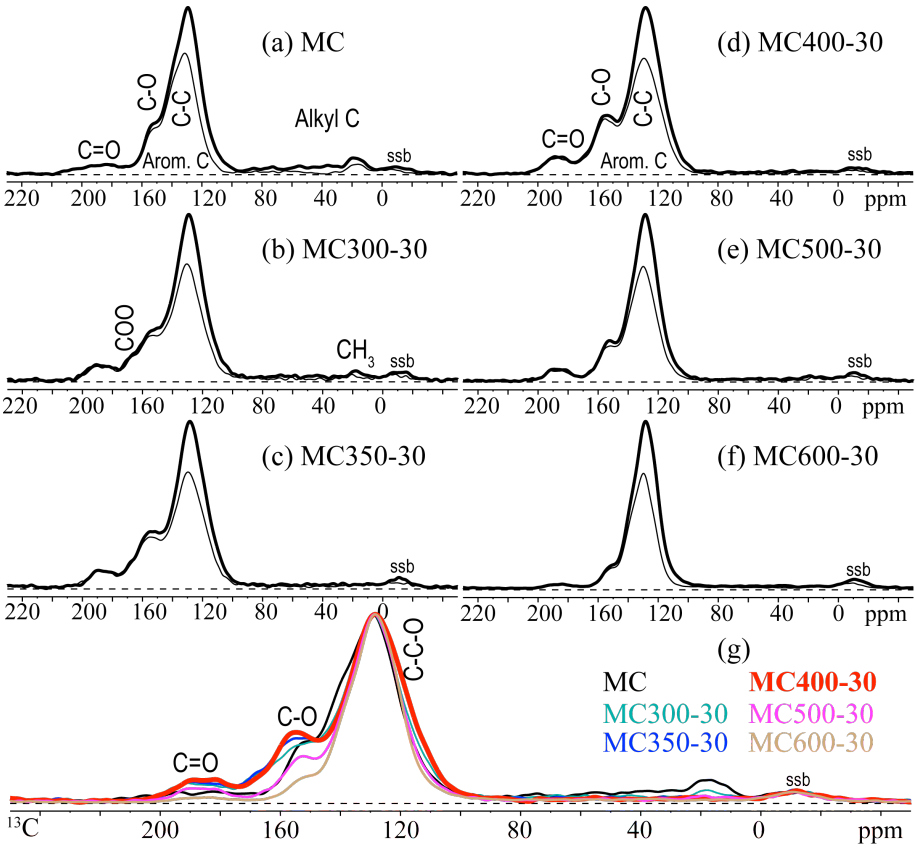

Figure 1. Nearly quantitative multiCP ^{13}C NMR spectra of maple wood chars treated by PPAO at different temperatures. Thick line: all C; thin line: nonprotonated C as well as CH_3. (a) MC, (b-f) MC PPAO-treated at 300, 350, 400, 500, and 600 ºC for 30 minutes, and (g) overlay of spectra of all samples to facilitate comparison. The spectra were scaled to match the intensity of the aromatic C band. 'ssb': spinning sideband.

A shoulder resonating between 160-170 ppm in the spectra of MC300-30 and MC350-30 corresponds to carboxyl (COO) groups. It is better resolved in the spectra after TOSS at 4 kHz MAS and dipolar dephasing, which suppresses the aromatic-carbon resonances; see Figure 2. With this spectral editing, the COO peak of MC300-30 (Fig. 2b) produces a discernable maximum.

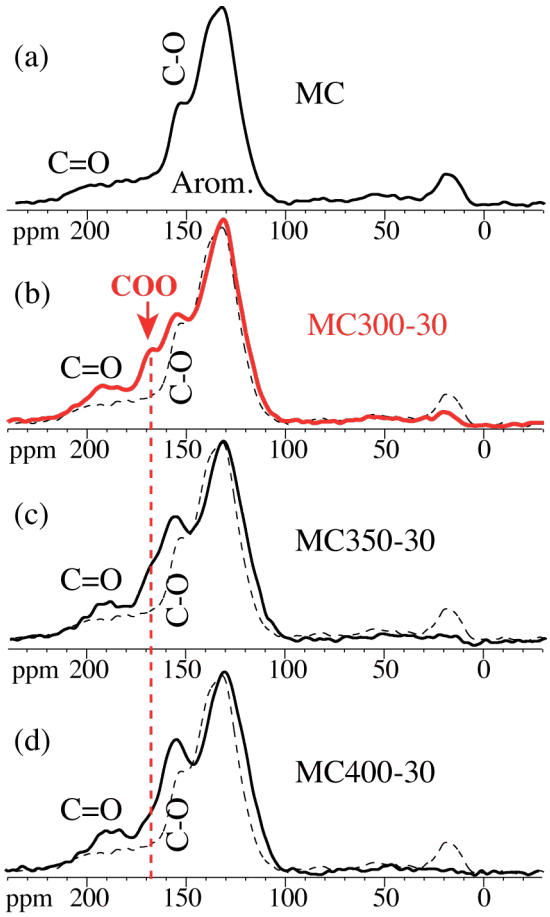

Figure 2. Selective ^{13}C NMR spectra of maple wood chars treated by PPAO at different temperatures, with COO bands enhanced relative to aromatic carbon signals by TOSS at 4 kHz MAS and dipolar dephasing. (a) MC without PPAO. This spectrum is shown as a dashed reference in the following three panels. (b-d) MC PPAO-treated for 30 minutes at (b) 300 ºC, (c) 350 ºC, and (d) 400 ºC. The spectra have been scaled to equal maximum peak height.

Quantification of functional groups showed that compared to untreated MC the relative abundances of aromatic C-O/COO increased in MC300-30, reached a maximum in MC350-30 chars, and decreased sharply in MC500-30 and MC600-30 (Fig. 3). The trend for C=O groups was similar, but the maximum appeared at slightly higher temperature (MC400-30). Nonoxygenated aromatic C including protonated aromatic C (Arom. C-H) and C-bonded

aromatic C (Arom. C-C) was unchanged below 400 ºC, but then increased markedly in MC500-30 and MC600-30. Interestingly, the alkyl C content decreased to a low minimum in MC400-30 and then appeared to increase slightly at the two higher temperatures. Overall, the results show that at 600 ºC, further pyrolysis rather than oxidation seemed to dominate.

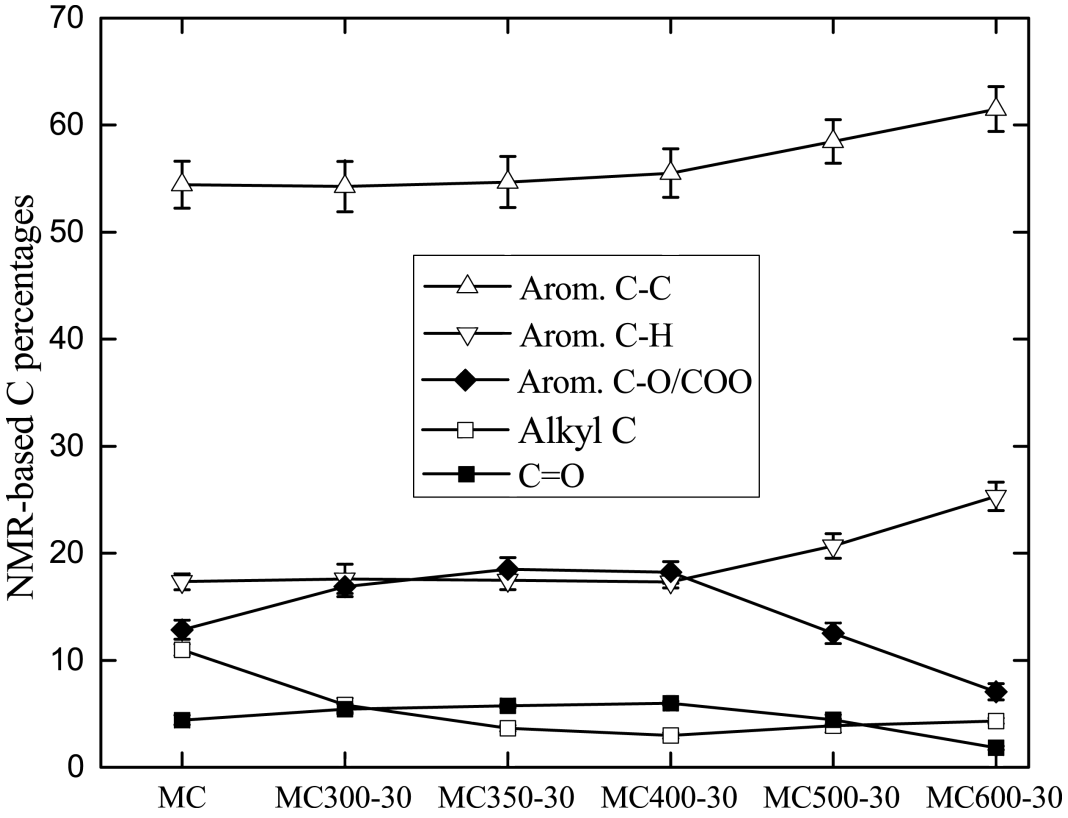

Figure 3. Plot of NMR-derived relative abundances of functional groups after PPAO for 30 min at increasing temperatures.

3.2. Effects of PPAO Time

The ^{13}C NMR spectra of maple wood chars PPAO-treated for different times at 400 ºC are shown in Fig. 4. The alkyl signals decreased strongly within the shortest treatment time (10 min; Fig. 4(a)). Compared to untreated maple wood char (MC), the relative abundances of aromatic C-O/COO and C=O increased, while that of alkyl C (mainly CH_3) decreased with PPAO time

(Figs. 4(e) and 5). These changes were smaller but more consistent than those observed for the temperature series (Fig. 1(g)).

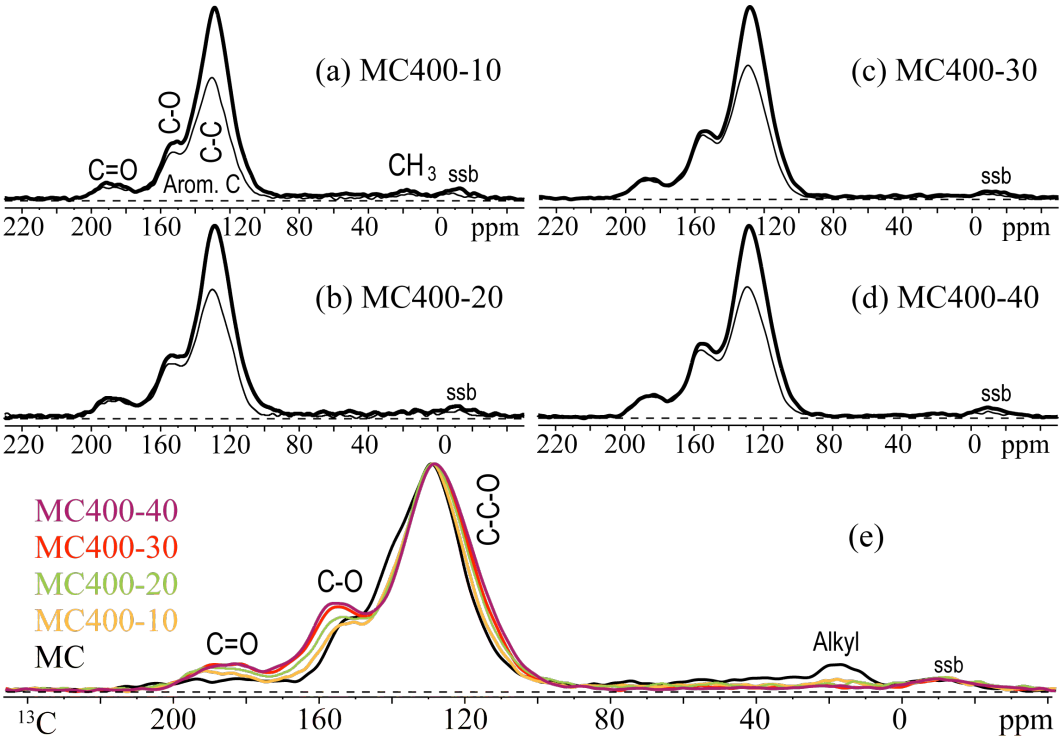

Figure 4. Nearly quantitative multiCP ^{13}C NMR spectra of maple wood chars treated at 400 ºC for (a) 10 min, (b) 20 min, (c) 30 min, and (d) 40 min. (e) Overlay of spectra of all samples to facilitate comparison. Thick line: all C; thin line: nonprotonated C as well as CH_3. The spectra were scaled to the same maximum peak height.

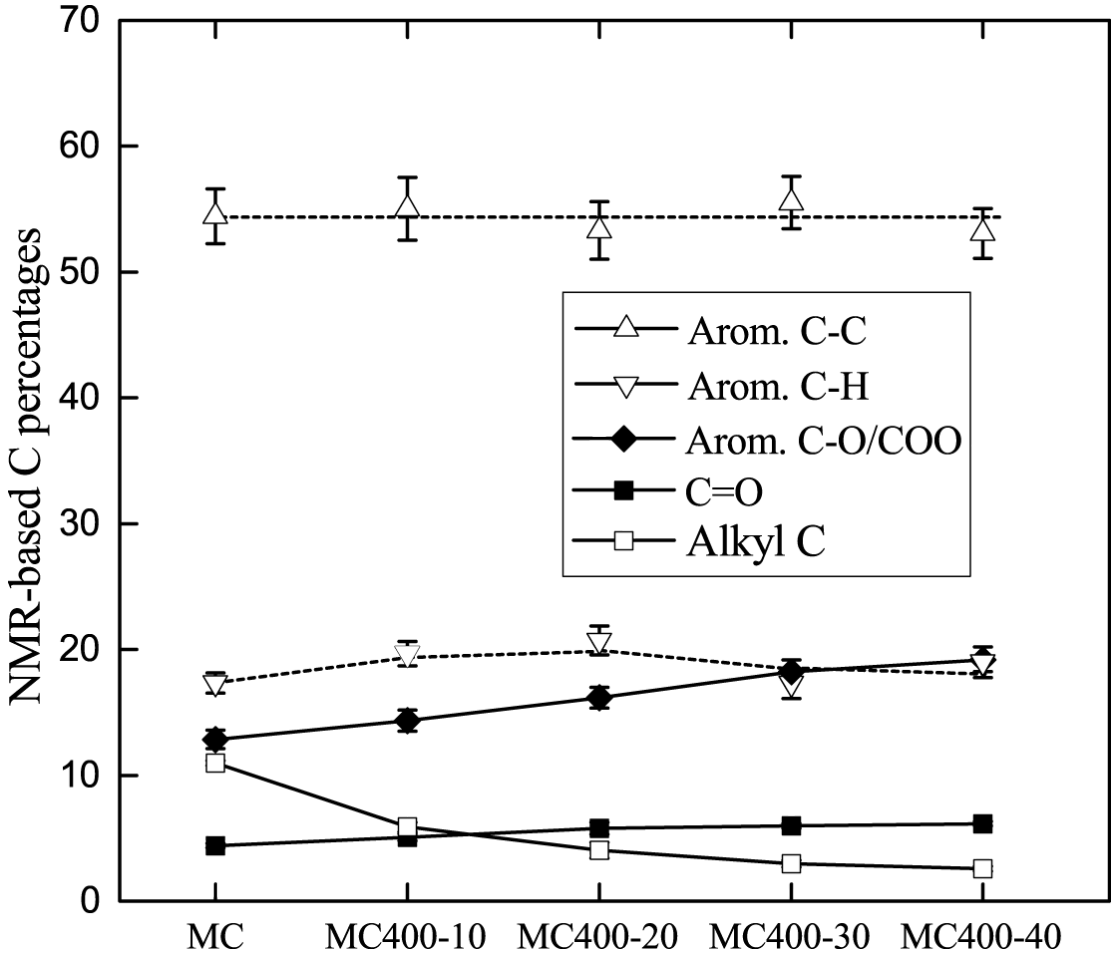

Figure 5. Plot of NMR-derived concentrations of functional groups as a function of duration of PPAO at 400 ºC.

Recoupled ^{1}H-^{13}C dipolar dephasing was applied to further identify changes in aromatic structures. The H-C dephasing of C-bonded aromatic C becomes progressively slower with increasing PPAO time (Fig. 6), a trend that is usually interpreted as an increase in aromatic cluster size. However, this trend may be also explained by extensive oxygen substitution occurring at the edge of the aromatic clusters, which removes hydrogens and increases the distance between interior aromatic carbons and their nearest hydrogens.

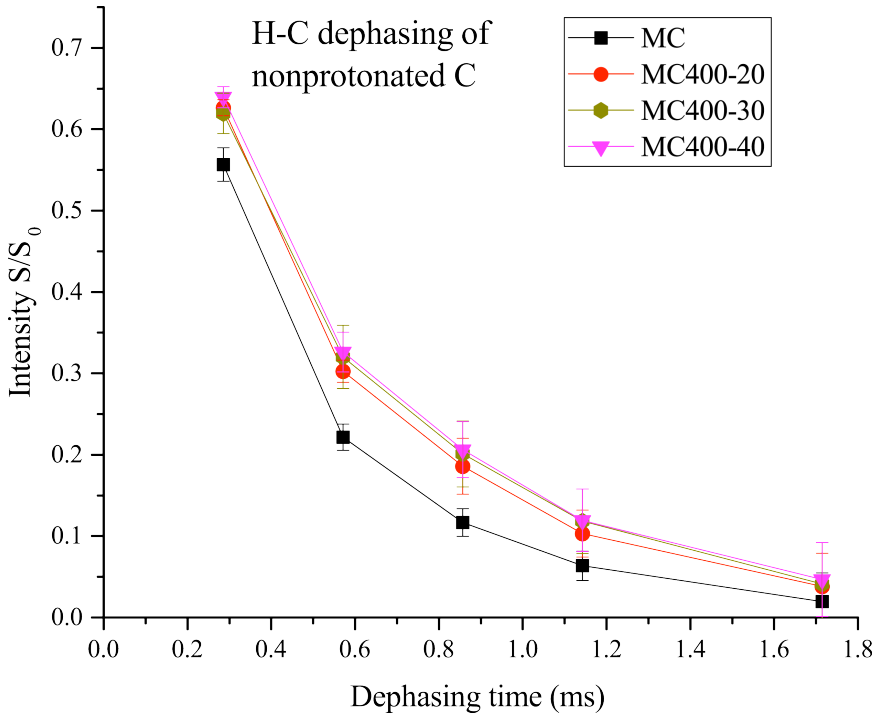

Figure 6. Plot of the area of ^{13}C NMR signals of nonprotonated aromatic carbons resonating between 107 and 142 ppm, under long-range ^{1}H-^{13}C dipolar dephasing.

3.3. Identification of Carboxyl Groups

Carboxyl groups attached to aromatic rings typically resonate near 170 ppm. While a COO peak is evident in spectra of pecan shell chars chemically oxidized by APS or HNO_3 (see Fig. 7), in agreement with the literature,[43] no similarly distinct band can be recognized in the NMR spectra of PPAO-treated chars, apart from a small shoulder at ~167 ppm for MC300-30, which is only revealed as a peak by TOSS selection (Fig. 2). Thus, a notable finding from this study is that the increase of carboxyl groups following PPAO treatment is not pronounced.

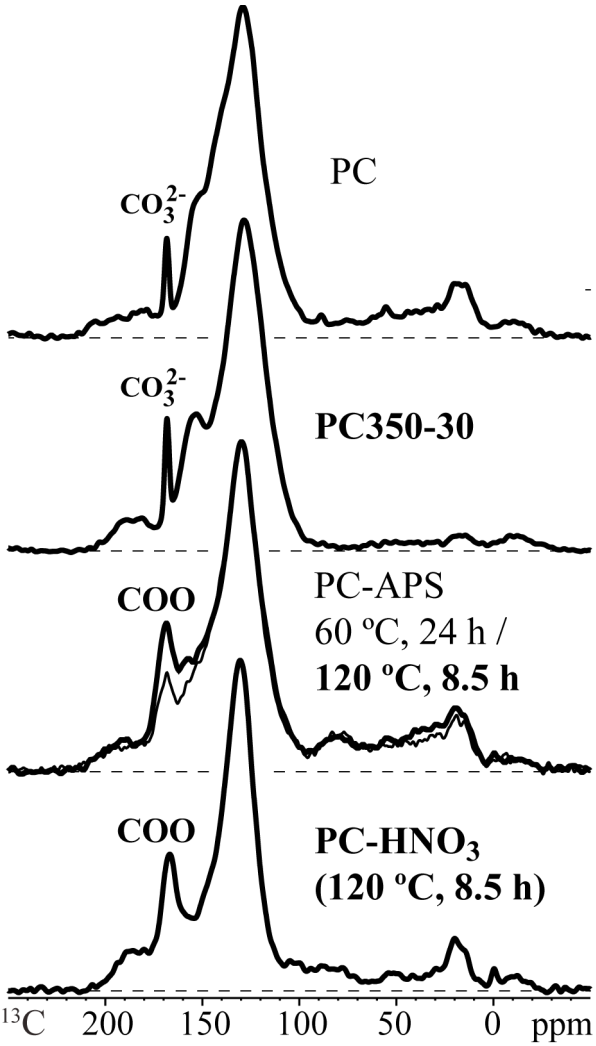

Figure 7. MultiCP ^{13}C NMR spectra of pecan shell chars (PC), PC treated by PPAO (PC350-30), and pecan shell chars chemically oxidized by APS (PC-APS) or HNO_3 (PC-HNO_3).

Based on results from potentiometric titration, Suliman et al.[21] concluded that air oxidation at 250 ºC for 30 min increased acidic functional groups, especially carboxyl on char surfaces. Xiao and Pignatello[24] concluded that air oxidation at 400 ºC for 30 min doubled the acidic functional groups, from 6.5 mequiv/g corresponding to ~1% carboxyl-C relative to total-C in untreated maple wood char, to 13 mequiv/g corresponding to ~2% of carboxyl-C relative to

285 total-C in the air-oxidized samples. These concentrations are consistent with the NMR
286 observation and indicate that thermal air oxidation of chars introduces fewer carboxyl groups
287 than does wet chemical oxidation.
288
289 **3.4. Identification of Carbonyl Groups**
290 The NMR spectra show that PPAO treatment remarkably increased carbonyl (ketone or quinone)
291 functionalities on chars. Previous studies of air-oxidized chars relying on titration or FT-IR
292 spectroscopy were not capable of identifying ketones/quinones. The broad carbonyl signals in
293 the 175-200 ppm region were retained after dipolar dephasing, indicating that they are in
294 nonprotonated C=O forms, i.e., ketone or quinone rather than aldehyde carbons. This relatively
295 low chemical shift range further indicates that the C=O moieties are bonded to aromatic
296 carbons.[40]
297
298 **3.5. Implications**
299 This study is among the first to show spectroscopically the identities and quantities of specific
300 oxygen functional groups introduced by exposure of biomass chars to hot air. The assignments of
301 C=O as well as C-O carbons and their structural environments can be further validated and
302 delineated with advanced two-dimensional ^{13}C-^{13}C NMR experiments of ^{13}C-labeled and PPAO-
303 treated glucose chars. Work along these lines is underway in our laboratories. Work is also in
304 progress to determine the structural changes induced by including air in the initial pyrolysis step,
305 as well as those induced by air oxidation under ambient conditions simulating aging in the
306 environment.

PPAO of biochars clearly does not result in the distinct structural features observed in chars that have undergone long-term oxidation in soils or chemical oxidation in controlled laboratory experiments. NMR analysis of char residues in soils[5] showed approximately 5 carboxylate carbons per 22 fused ring carbons; the level of carboxyl substitution is considerably higher than the levels found in the PPAO-treated chars of this study.

Introduction of oxygen functional groups by air oxidation has major implications for the interaction of char materials with nutrients, natural organic matter, pollutants, and microbes in soil. Carboxyl groups provide cation exchange capacity that helps regulate the retention and bioavailability of nutrient cations in soil. Moreover, carboxyl groups can undergo strong hydrogen bonding with weak acid and base functional groups of pollutants[9, 24, 44] and soil organic matter.[45] Keto and phenolic groups belonging to quinone/hydroquinone systems are thought to contribute to the electron donor-acceptor properties of chars,[46, 47], which may be linked to molecule-to-molecule, molecule-to-cell and cell-to-cell electron transfer processes.[9, 48]

ACKNOWLEDGMENTS

This work was funded by the National Science Foundation of the United States (grant CHE 1709532).

330 **REFERENCES**

[1] B. Glaser, L. Haumaier, G. Guggenberger, W. Zech, The'Terra Preta'phenomenon: a model for sustainable agriculture in the humid tropics, Naturwissenschaften 88 (1) (2001) 37-41

[2] M.W. Schmidt, A.G. Noack, Black carbon in soils and sediments: analysis, distribution, implications, and current challenges, Global Biogeochem. Cycles 14 (3) (2000) 777-793

[3] J.O. Skjemstad, D.C. Reicosky, A.R. Wilts, J.A. McGowan, Charcoal carbon in US agricultural soils, Soil Sci. Soc. Am. J. 66 (4) (2002) 1249-1255

[4] J. Skjernstad, J. Taylor, R. Smernik, Estimation of charcoal (char) in soils, Commun. Soil. Sci. Plant. Anal. 30 (15-16) (1999) 2283-2298

[5] J.-D. Mao, R. Johnson, J. Lehmann, D. Olk, E.G. Neves, M. Thompson, et al., Abundant and stable char residues in soils: implications for soil fertility and carbon sequestration, Environ. Sci. Technol. 46 (17) (2012) 9571-9576

[6] D.A. Laird, The charcoal vision: a win–win–win scenario for simultaneously producing bioenergy, permanently sequestering carbon, while improving soil and water quality, Agron. J. 100 (1) (2008) 178-181

[7] J. Lehmann, S. Joseph, Biochar for environmental management: science, technology and implementation, Routledge, 2015.

[8] L. Van Zwieten, C. Kammann, M.L. Cayuela, B.P. Singh, S. Joseph, S. Kimber, et al., Biochar effects on nitrous oxide and methane emissions from soil, Biochar for environmental management: science and technology. 2nd ed. London, New York: Earthscan Books Ltd (2015) 489-520

[9] J. Pignatello, W.A. Mitch, W. Xu, Activity and reactivity of pyrogenic carbonaceous matter toward organic compounds, Environ. Sci. Technol. 51 (16) (2017) 8893-8908

[10] L.C. Bornemann, R.S. Kookana, G. Welp, Differential sorption behaviour of aromatic hydrocarbons on charcoals prepared at different temperatures from grass and wood, Chemosphere 67 (5) (2007) 1033-1042

[11] Y. Chun, G. Sheng, C.T. Chiou, B. Xing, Compositions and sorptive properties of crop residue-derived chars, Environ. Sci. Technol. 38 (17) (2004) 4649-4655

[12] C. Lattao, X. Cao, J. Mao, K. Schmidt-Rohr, J.J. Pignatello, Influence of molecular structure and adsorbent properties on sorption of organic compounds to a temperature series of wood chars, Environ. Sci. Technol. 48 (9) (2014) 4790-4798

[13] F. Xiao, J.J. Pignatello, Interactions of triazine herbicides with biochar: Steric and electronic effects, Water Res. 80 (2015) 179-188

[14] S.M. Martin, R.S. Kookana, L. Van Zwieten, E. Krull, Marked changes in herbicide sorption–desorption upon ageing of biochars in soil, J. Hazard. Mater. 231 (2012) 70-78

[15] C.E. Brewer, E.T. Hall, K. Schmidt‐Rohr, D.A. Laird, R.C. Brown, K. Zygourakis, Temperature and reaction atmosphere effects on the properties of corn stover biochar, Environ. Prog. Sustain. Energy 36 (3) (2017) 696-707

[16] N. Gil-Lalaguna, J. Sánchez, M. Murillo, V. Ruiz, G. Gea, Air-steam gasification of char derived from sewage sludge pyrolysis. Comparison with the gasification of sewage sludge, Fuel 129 (2014) 147-155

[17] N. Mahinpey, P. Murugan, T. Mani, R. Raina, Analysis of bio-oil, biogas, and biochar from pressurized pyrolysis of wheat straw using a tubular reactor, Energy Fuels 23 (5) (2009) 2736-2742

[18] H. Oda, M. Takeuchi, C. Yokokawa, Effect of air-oxidation on the pore-structure of coals and cokes or chars obtained from oxidized coals, Fuel 60 (5) (1981) 390-396

[19] J. Pis, T.A. Centeno, M. Mahamud, A.B. Fuertes, J. Parra, J.A. Pajares, et al., Preparation of active carbons from coal Part I. Oxidation of coal, Fuel Process. Technol. 47 (2) (1996) 119-138

[20] M.S. Tam, M.J. Antal, Preparation of activated carbons from macadamia nut shell and coconut shell by air activation, Ind. Eng. Chem. Res. 38 (11) (1999) 4268-4276

[21] W. Suliman, J.B. Harsh, N.I. Abu-Lail, A.-M. Fortuna, I. Dallmeyer, M. Garcia-Perez, Modification of biochar surface by air oxidation: Role of pyrolysis temperature, Biomass Bioenergy 85 (2016) 1-11

[22] A. Koch, A. Krzton, G. Finqueneisel, O. Heintz, J.-V. Weber, T. Zimny, A study of carbonaceous char oxidation in air by semi-quantitative FTIR spectroscopy, Fuel 77 (6) (1998) 563-569

[23] F. Xiao, A.H. Bedane, J.X. Zhao, M.D. Mann, J.J. Pignatello, Thermal air oxidation changes surface and adsorptive properties of black carbon (char/biochar), Sci. Total Environ. 618 (2018) 276-283

[24] F. Xiao, J.J. Pignatello, Effects of post-pyrolysis air oxidation of biomass chars on adsorption of neutral and ionizable compounds, Environ. Sci. Technol. 50 (12) (2016) 6276-6283

[25] V.N. Tsaneva, W. Kwapinski, X. Teng, B.A. Glowacki, Assessment of the structural evolution of carbons from microwave plasma natural gas reforming and biomass pyrolysis using Raman spectroscopy, Carbon 80 (2014) 617-628

[26] G. Levi, O. Senneca, M. Causà, P. Salatino, P. Lacovig, S. Lizzit, Probing the chemical nature of surface oxides during coal char oxidation by high-resolution XPS, Carbon 90 (2015) 181-196

[27] R.L. Johnson, K. Schmidt-Rohr, Quantitative solid-state 13C NMR with signal enhancement by multiple cross polarization, J. Magn. Reson. 239 (2014) 44-49

[28] P. Duan, K. Schmidt-Rohr, Composite-pulse and partially dipolar dephased multiCP for improved quantitative solid-state 13 C NMR, J. Magn. Reson. 285 (2017) 68-78

[29] J.-D. Mao, K. Schmidt-Rohr, Recoupled long-range C–H dipolar dephasing in solid-state NMR, and its use for spectral selection of fused aromatic rings, J. Magn. Reson. 162 (1) (2003) 217-227

[30] T.M. Duncan, Principal Components of Chemical Shift Tensors: A Compilation, Farragut Press, 1997.

[31] Z. Gu, A. McDermott, Chemical shielding anisotropy of protonated and deprotonated carboxylates in amino acids, J. Am. Chem. Soc. 115 (10) (1993) 4282-4285

[32] L.A. Langley, D.H. Fairbrother, Effect of wet chemical treatments on the distribution of surface oxides on carbonaceous materials, Carbon 45 (1) (2007) 47-54

[33] C.E. Brewer, K. Schmidt-Rohr, J.A. Satrio, R.C. Brown, Characterization of biochar from fast pyrolysis and gasification systems, Environ. Prog. Sustain. Energy 28 (3) (2009) 386-396

[34] A. Vyalikh, V.O. Koroteev, W. Münchgesang, T. Köhler, C. Röder, E. Brendler, et al., Effect of Charge Transfer upon Li- and Na-Ion Insertion in Fine-Grained Graphitic Material as Probed by NMR, ACS Appl. Mater. Interfaces 11 (9) (2019) 9291-9300

[35] R.E. Franklin, J.T. Randall, Crystallite growth in graphitizing and non-graphitizing carbons, Proc. R. Soc. Lond. A Math. Phys. Sci. 209 (1097) (1951) 196-218

[36] A. Oberlin, Pyrocarbons, Carbon 40 (1) (2002) 7-24

[37] X. Fang, J. Mao, E. Levin, K. Schmidt-Rohr, Nonaromatic core− shell structure of nanodiamond from solid-state NMR spectroscopy, J. Am. Chem. Soc. 131 (4) (2009) 1426-1435

[38] J.-W. Feng, S. Zheng, G.E. Maciel, EPR investigations of charring and char/air interaction of cellulose, pectin, and tobacco, Energy Fuels 18 (2) (2004) 560-568

[39] R.J. Smernik, J.M. Oades, The use of spin counting for determining quantitation in solid state 13C NMR spectra of natural organic matter: 2. HF-treated soil fractions, Geoderma 96 (3) (2000) 159-171

[40] R.L. Johnson, J.M. Anderson, B.H. Shanks, X. Fang, M. Hong, K. Schmidt-Rohr, Spectrally edited 2D ^{13}C-^{13}C NMR spectra without diagonal ridge for characterizing ^{13}C-enriched low-temperature carbon materials, J. Magn. Reson. 234 (2013) 112-124

[41] W. Dixon, J. Schaefer, M. Sefcik, E. Stejskal, R. McKay, Total suppression of sidebands in CPMAS C-13 NMR, J. Magn. Reson. 49 (2) (1982) 341-345

[42] J.M. Anderson, R.L. Johnson, K. Schmidt-Rohr, B.H. Shanks, Solid state NMR study of chemical structure and hydrothermal deactivation of moderate-temperature carbon materials with acidic SO_3H sites, Carbon 74 (2014) 333-345

[43] L. Haumaier, W. Zech, Black carbon—possible source of highly aromatic components of soil humic acids, Org. Geochem. 23 (3) (1995) 191-196

[44] X. Li, J.J. Pignatello, Y. Wang, B. Xing, New insight into adsorption mechanism of ionizable compounds on carbon nanotubes, Environ. Sci. Technol. 47 (15) (2013) 8334-8341

[45] J. Ni, J.J. Pignatello, Charge-assisted hydrogen bonding as a cohesive force in soil organic matter: water solubility enhancement by addition of simple carboxylic acids, Environ. Sci. Processes Impacts 20 (9) (2018) 1225-1233

[46] L. Klüpfel, M. Keiluweit, M. Kleber, M. Sander, Redox properties of plant biomass-derived black carbon (biochar), Environ. Sci. Technol. 48 (10) (2014) 5601-5611

[47] T. Sun, B.D. Levin, J.J. Guzman, A. Enders, D.A. Muller, L.T. Angenent, et al., Rapid electron transfer by the carbon matrix in natural pyrogenic carbon, Nat. Commun. 8 (2017) 14873

[48] A. Kappler, M.L. Wuestner, A. Ruecker, J. Harter, M. Halama, S. Behrens, Biochar as an electron shuttle between bacteria and Fe (III) minerals, Environ. Sci. Technol. Lett. 1 (8) (2014) 339-344